Dioxovanadium(V) Complexes of ONO Donor Ligands Derived from Pyridoxal and Hydrazides: Models of Vanadate-Dependent Haloperoxidases

Mannar R. Maurya,*[a] Shalu Agarwal,[a] Cerstin Bader,[b] and Dieter Rehder*[b]

Keywords: Vanadium / Hydrazones / Catalytic bromination / Pyridoxal

[VO(acac)$_2$] reacts with H_2L [H_2L are the hydrazones H_2pydx-inh (**I**), H_2pydx-nh (**II**), or H_2pydx-bhz (**III**); pydx = pyridoxal, inh = isonicotinohydrazide, nh = nicotinohydrazide, bhz = benzohydrazide] in dry methanol to yield the oxovanadium(IV) complexes [VOL] (H_2L = **I**: **1**; H_2L = **II**: **4**) or [VO(pydx-bhz)]. These complexes, when exposed to air, convert into the corresponding dioxovanadium(V) complexes [VO_2HL] (H_2L = **I**: **2**; H_2L = **II**: **5**; H_2L = **III**: **7**). Aqueous solutions of vanadate and the ligands at pH = 7.5 give rise to the formation of [K(H_2O)$_3$][VO_2(pydx-inh)] (**3**), [K(H_2O)$_2$][VO_2-(pydx-nh)] (**6**) and [K(H_2O)$_2$][VO_2(pydx-bhz)] (**8**). Treatment of **6** and **8** with H_2O_2 generates the oxo(peroxo)vanadium complexes [VO(O_2)L] (H_2L = **II**: **9**; H_2L = **III**: **10**). Complexes **9** and **10** are capable of transferring an oxo group to PPh_3. Acidification of **8** with HCl afforded a hydroxo(oxo) complex. The crystal and molecular structures of ligand **I** and complex **3** have been solved by single-crystal X-ray diffraction. In the anion **3**, the vanadium atom is in a distorted tetragonal-pyramidal environment (τ = 0.23). The K^+ ion is coordinated to four water molecules (two of which bridge to a neighbouring K^+ ion), the pyridine nitrogen atom of an isonicotinic moiety, the equatorial oxo group of the VO_2^+ fragment, and the alcoholic group of the pyridoxal moiety, which links adjacent layers in the three-dimensional lattice network. In the presence of KBr/H_2O_2, the anionic complexes **3**, **6** and **8** catalyse the oxidative bromination of salicylaldehyde in water to 5-bromosalicylaldehyde in ca. 40% yields with ca. 87% selectivity.

Introduction

Recent interest in vanadium coordination chemistry[1,2] with *ON* oligodentate ligands arises from the potential of these complexes as insulin-enhancing or insulin-mimetic agents,[3] their model character for vanadate-dependent haloperoxidases occurring in fungi and marine algae[4] and, in relation to these enzymes, their use in oxo-transfer catalysis and oxidative halogenation. Vanadate-dependent haloperoxidases contain VO(OH)O_2^{2-} (HVO_4^{2-}) coordinated to the N^{ε} of a histidine in an overall trigonal-bipyramidal coordination.[5] These enzymes, and models of their active centre, catalyse the oxidation of halides by peroxide to hypohalous acid [which further halogenate non-enzymatically hydrocarbons; Equation (1)],[6] and the oxidation of organic (prochiral) sulfides to (chiral) sulfoxides.[7,8] Peroxo and hydroperoxo complexes have been proposed to act as the active intermediates.[6,9] The peroxo form, containing peroxovanadate $HVO_3(O_2)^{2-}$ attached to histidine, and in a tetragonal-pyramidal geometry, has been structurally characterised.[10]

$$Hal^- + H_2O_2 + RH + H^+ \rightarrow RHal + 2\,H_2O \quad (1)$$

We have previously reported on dioxovanadium(V) complexes with *ONO*, *NNO* and *NNS* functional ligands, derived from hydrazones based on the carbonyl components salicylaldehyde or 2-acetylpyridine, and the hydrazides of isonicotinic or benzoic acid, or *S*-benzyldithiocarbazate,[11] and reduced Schiff bases derived from salicylaldehyde and various amino acids.[12] Anionic and neutral *cis*-dioxovanadium(V) complexes with tridentate (*ONO*) *N*-salicylidenehydrazide ligand systems as models for vanadate-dependent haloperoxidases have recently been reviewed by Plass.[13] The present work is an extension to hydrazones formed from the biogenic carbonyl constituents pyridoxal (vitamin B_6; HpydxOH), and the hydrazides of nicotinic acid (H_2nh), isonicotinic acid (H_2inh) or benzoic acid (H_2bhz; see Scheme 1), which reveals novel structural features, and reactivity patterns that model the haloperoxidase activity.

Results and Discussion

Scheme 2 provides an overview of the complexes reported in this contribution. Structures of these complexes are based on spectroscopic (IR, UV/Vis, EPR, ^{1}H and ^{51}V NMR) data, thermogravimetric studies, elemental analyses and X-ray diffraction analyses of the ligand H_2pydx-inh (**I**) and complex **3**.

[a] Department of Chemistry, Indian Institute of Technology Roorkee,
Roorkee 247667, India
E-mail: rkmanfcy@iitr.ernet.in
[b] Institut für Anorganische und Angewandte Chemie, Universität Hamburg,
Martin-Luther-King-Platz 6, 20146 Hamburg, Germany
E-mail: dieter.rehder@chemie.uni-hamburg.de

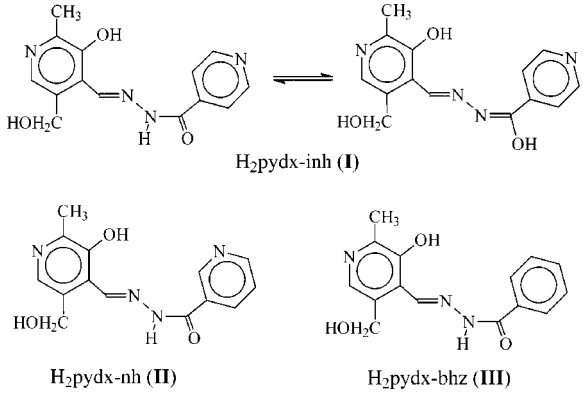

Scheme 1. Tautomerism shown for **I** only

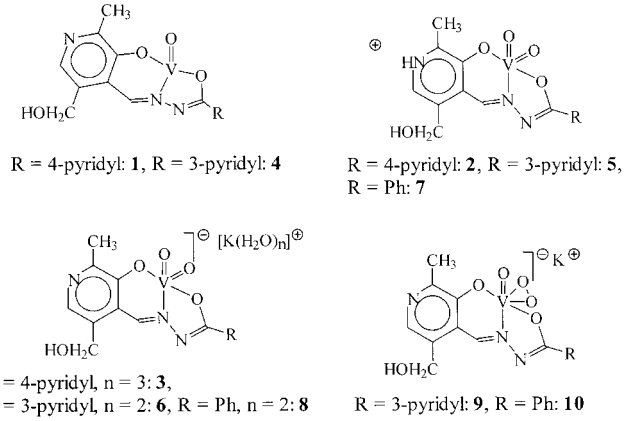

Scheme 2. **1** and **4** are idealised structural units; cf. text

Synthesis and General Characteristics

Reaction between equimolar amounts of $[VO(acac)_2]$ and ligand **I** or **II** (Scheme 1) in dry, refluxing methanol gave the oxovanadium(IV) complex [VO(pdyx-inh)] (**1**) or [VO(pdyx-nh)] (**4**), respectively. According to elemental analyses and thermogravimetric studies, there is no coordinated additional ligand such as water or methanol present in the isolated, solid compounds; **1** and **4** exhibit a magnetic moment, at ambient temperature of 1.32 and 1.41 μ_B, respectively; the spin-only value for a d^1 system is 1.73 μ_B. The magnetic data can be interpreted in terms of antiferromagnetic exchange interaction,[14] implying close contacts between the monomers or the formation of dinuclear complexes such as $[\{VO(L)\}_2\mu\text{-}O]$. Although dinuclear complexes of this type are well documented,[15] the size of the magnetic moments and the low wave number for the V=O stretch (888 cm^{-1}) suggest intermolecular interactions of the kind (L)V=O···VO(L),[16] and thus an effective coordination number of 5. Anisotropic EPR data of DMSO solutions (see Exp. Sect.) correspond to those expected for the equatorial donor set shown for **1** and **4** in Scheme 2, i.e. $O_{phenolate}N_{imine}O_{enolate}$, plus a relatively weakly bonding equatorial ligand such as water or DMSO.[17]

On aerial oxidation of **1** in methanol, the dioxovanadium(V) complex $[VO_2(Hpdyx\text{-}inh)]$ (**2**) was obtained. The intermediate complex **1** can be isolated from the methanolic solution prior to aeration. Equations (2) and (3) represent the synthetic procedures.

$$\underset{\mathbf{I}}{[VO(acac)_2]} + H_2pydx\text{-}inh \rightarrow \underset{\mathbf{1}}{[V^{IV}O(pydx\text{-}inh)]} + 2\ Hacac \quad (2)$$

$$\underset{\mathbf{1}}{2\ [VO(pydx\text{-}inh)]} + H_2O + 1/2\ O_2 \rightarrow \underset{\mathbf{2}}{2\ [V^{V}O_2(Hpydx\text{-}inh)]} \quad (3)$$

Similarly, the complex [VO(pydx-nh)] (**4**), can be oxidised in methanol to $[VO_2(Hpydx\text{-}nh)]$ (**5**). Further, complexes **2** and **5** were obtained from the reaction of potassium vanadate (which, at ambient pH, is actually present as a mixture of vanadates; vide infra), generated in situ by dissolving V_2O_5 in an aqueous solution of KOH, with solutions of the potassium salts of ligands **I** or **II** and adjustment of the pH of the reaction mixture to 6.0. Adjustment of the pH of these solutions to 7.5 results in the formation of a mixture of $[K(H_2O)_3][VO_2(pydx\text{-}inh)]$ (**3**) and **2** [Equation (4)], or $[K(H_2O)_2][VO_2(pydx\text{-}nh)]$ (**6**) and **5**, respectively. The final pH of the reaction mixture plays an important role in that a decrease in pH (e.g. to pH = 6.5) increases the yield of the neutral complexes **2** or **5**. This pH dependence is possibly due to the actual vanadate species present in solution: At pH = 6, $H_2VO_4^-$ is in equilibrium with $H_2V_2O_7^{2-}$, $V_4O_{12}^{4-}$(dominant species), $V_5O_{15}^{5-}$ and $V_{10}O_{28}^{6-}$; at pH = 7.5, decavanadate disappears, and monovanadate (again in equilibrium with divanadate, tetravanadate as the main species, and pentavanadate) is present in the mono- and diprotonated forms (the pK_a for $H_2VO_4^-$ is around 8.1).[18] The two complexes **2** and **3**, or **5** and **6**, can be separated by fractional crystallisation from methanol, where the neutral complex crystallises first. Complexes **7** and **8** were prepared similarly from $[VO(acac)_2]$ and "KVO_3", respectively. Addition of H_2O_2 to the methanolic solution of **6** and **7** yields the oxomono(peroxo)vanadium(V) complexes **9** and **10** [Equation (5)].

$$K_{3-x}H_xVO_4 + K_2pydx\text{-}inh \rightarrow \underset{\mathbf{2}}{[VO_2(Hpydx\text{-}inh)]} + \underset{\mathbf{3}}{[K(H_2O)_3][VO_2(pydx\text{-}inh)]}\ (x = 1, 2) \quad (4)$$

$$[VO_2L]^- + H_2O_2 \rightarrow [VO(O_2)L]^- + H_2O \quad (H_2L = \mathbf{II}: \mathbf{9};\ H_2L = \mathbf{III}: \mathbf{10}) \quad (5)$$

Potassium vanadate reacts with 30% aqueous H_2O_2 to generate $K[VO(O_2)_2(OH/H_2O)_x]^{n-}$. In the presence of the potassium salt of ligand **III**, the peroxo complex $K[VO(O_2)(pydx\text{-}bhz)]$ (**10**) forms; see idealised Equation (6).

$$KH_2VO_4 + K_2pydx\text{-}bhz + H_2O_2 \rightarrow K[VO(O_2)(pydx\text{-}bhz)] + 2\ KOH + H_2O \quad (6)$$

The peroxo complex of ligand **I** could not be isolated in the solid state by any of the above methods due to its instability at ambient temperature. The formation of a peroxo complex in solution by treatment of **8** with H_2O_2 has also

been established by electronic absorption spectroscopy. The spectral changes are depicted in Figure 1. The band for $[VO_2(pydx\text{-}bhz]^-$ (**8**) at 404.5 nm shifts to 424 nm along with an increase in intensity on dropwise addition of H_2O_2, while the band at 329 nm only marginally shifts to 333 nm with partial reduction in intensity. The amount of peroxo complex formed depends upon the amount of H_2O_2 added. The final spectral pattern is similar to that obtained for the isolated peroxo complex **10** in methanol.

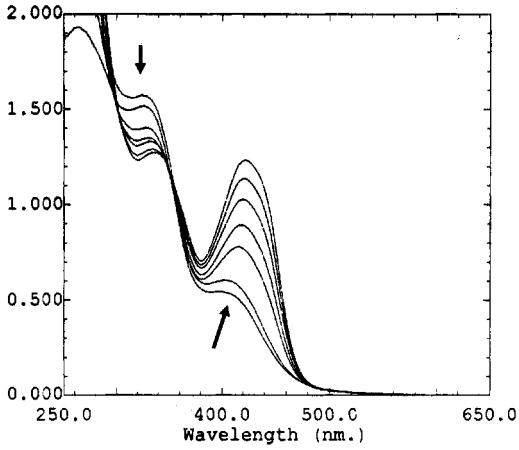

Figure 1. Titration of $[K(H_2O)_2][VO_2(pydx\text{-}bhz)]$ (**8**) with 30% H_2O_2; the spectra were recorded after successive addition of 2-drop portions of H_2O_2 to 10 mL of a ca. 10^{-4} M solution of **8** in MeOH

The peroxo complexes **9** and **10** undergo oxygen transfer reactions with PPh_3 in methanol to give the corresponding dioxovanadium(V) complexes **6** and **8** [Equation (7)].

$$[VO(O_2)L]^- + PPh_3 \rightarrow [VO_2L]^- + OPPh_3;\ (H_2L = \mathbf{I} \text{ or } \mathbf{III}) \quad (7)$$

Structure Description

An ORTEP plot and cell drawing of the ligand H_2pydx-inh (**I**) along with the atom-labelling scheme is presented in Figure 2 and selected structure parameters in Table 1. The bond parameters are well within the expected range. From the bond lengths *d*(C6−O1) [1.223(2) Å] and *d*(C6−N2) [1.363(3) Å], and the angles at C6 (av.120.0°) and N2 [116.0(2)°] it is clear that in the free ligand the ketonic form

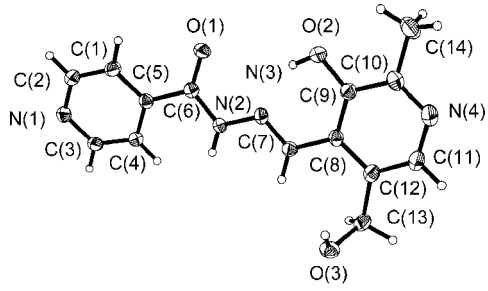

Figure 2. ORTEP plot (at the 50% probability level) of the ligand H_2pydx-inh (**I**)

Table 1. Bond lengths [Å] and angles [°] for **I** and **3** (symmetry transformations used to generate equivalent atoms: #1: $-x, -y + 1, -z$; #2: $x, y + 1, z$; #3: $x, y - 1, z$; #4: $x, y, z + 1$)

I		**3**	
		V1−O1	1.6318(12)
		V1−O2	1.6332(12)
		V1−O3	1.9906(11)
		V1−O4	1.8886(11)
		V1−N3	2.1233(13)
		K1−O2	2.8309(12)
		K1−O5	2.7184(13)
		K1−O6	2.8867(13)
		K1−O7	2.9463(13)
		K1−O8	2.7893
		K1−O8#	2.8444(14)
		K1−N1	2.8076(14)
		K1···K1#	3.8176
O1−C6	1.223(3)	O3−C6	1.3053(18)
N2−C6	1.363(3)	N2−C6	1.302(2)
N2−N3	1.362(3)	N2−N3	1.3969(18)
N3−C7	1.281(3)	N3−C7	1.2984(19)
O2−C9	1.354(3)	O4−C12	1.3185(18)
C12−C13	1.506(3)	C9−C14	1.510(2)
O3−C13	1.428(3)	O5−C14	1.427(2)
		O2−V1−N3	138.99(6)
		O3−V1−O4	152.65(5)
		O3−V1−N3	73.91(5)
		O4−V1−N3	82.40(5)
		V1−O2−K1	133.64(7)
		O2−K1−O5	156.19(4)
		K1−O5−C14	128.30(10)
		K1−O8−K1#	85.31(4)
C12−C13−O3	113.5(2)	C9−C14−O5	110.29(13)
O1−C6−N2	122.7(2)	O3−C6−N2	123.48(14)
C6−N2−N3	116.0(2)	C6−N2−N3	108.45(12)
N3−C7−C8	117.7(2)	N3−C7−C8	124.02(14)

prevails. This is further confirmed by an intermolecular hydrogen bond N2H···O3HCH$_2$ (1.970 Å). Additional close intermolecular contacts exist between adjacent molecules via C3H and O1 (2.575 Å) of the isonicotinic acid moieties, as well as isonicotinic N1 and pyridoxal O3HCH$_2$ (2.749 Å).

Figure 3 shows an ORTEP plot and a schematic drawing for the vanadium and potassium coordination environments of **3**; Figure 4 is a representation of the 3D arrangement of the molecular units. Selected structure parameters are collated in Table 1. The geometry of the anion can be described in terms of a tetragonal pyramid, distorted towards a trigonal bipyramid. The τ value {[∠(O3−V−O4) − ∠(O2−V−N3)]/60} is 0.23 (τ = 0 vs. 1 for ideal tetragonal-pyramidal vs. trigonal-bipyramidal arrangements), reflecting a common situation encountered with pentacoordinate oxovanadium complexes. For rare examples of a distorted trigonal-bipyramidal arrangement, see ref.[19] The *cis*-dioxovanadium unit is coordinated through the phenolate oxygen atom O4 of pyridoxal, the imine nitrogen atom N3, and the enolate oxygen atom O3 of the isonicotinic acid hydrazone. Together with the doubly bonded O2, bridging to the potassium ion, these functions form the tetragonal plane. The angle at O2 is 133.67(7)°. The bond lengths

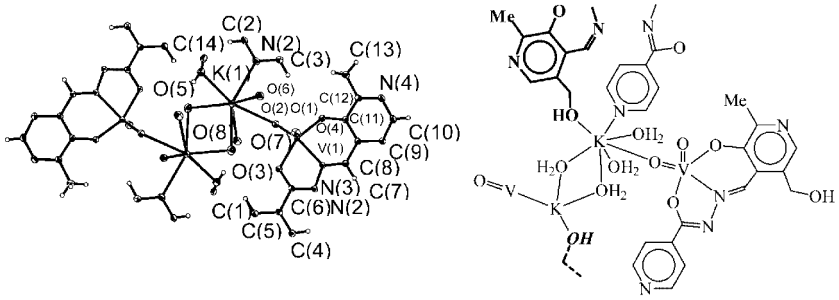

Figure 3. ORTEP plot (30% probability level) of $[K(H_2O)_3](VO_2(pydx\text{-}inh)]$ (**3**), and a schematic drawing of the vanadium and potassium environments; bold parts refer (to connections) to planes above and below

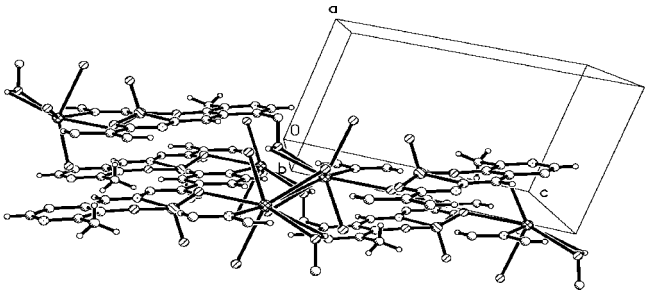

Figure 4. Section from the crystal lattice of **3**, showing the supramolecular arrangement

d(V−N3) [2.1233(13)], *d*(V−O3) [1.9906(11)] and *d*(V−O4) [1.8886(11) Å] are in agreement with literature values for imine, enolate and phenolate coordinating to the vanadium centre. Further, the bond lengths *d*(N2−N3) [1.3969(18)], *d*(N2−C6) [1.302(17)] and *d*(O3−C6) [1.3053(18) Å] are consistent with the enolate mode of coordination, supported by a comparison with the respective parameters for the free ligand (Table 1), in which the carbonyl form is present. The apical V=O bond, *d*(V−O1) = 1.6318(12) is in the expected range, while the basal V=O bond, *d*(V−O2) = 1.66332(12) Å, is slightly elongated as a consequence of covalent bonding contact to the K^+ ion.

The K^+ ion links three complex anions through the basal oxo group of VO_2^+ (O2), the pyridine nitrogen atom of an isonicotinic acid moiety (N1) and the alcoholic oxygen atom of a pyridoxal moiety (O5). In addition, four water molecules (three per molecular unit) are coordinated to K^+, resulting in the coordination number 7 for each potassium ion. In the dinuclear rhombohedral $\{K_2(\mu\text{-}OH_2)_2\}$ core, the angles are 85.31(4) at O8 and 94.69(4)° at K1; *d*(K1···K1#) amounts to 3.818 Å. O5 on K1 and O5# on K1# link to adjacent planes. Supramolecular links are further established by one of the terminal water molecules, which is hydrogen-bonded to the ring nitrogen atom of the pyridoxal moiety, N4···H_2O6 = 2.848 Å.

For the structures of the related complexes **2**, **5** and **7**, **6** and **8**, and the peroxo complexes **9** and **10**, we assume a ligand arrangement corresponding to that in **3**; cf. Scheme 2.

Thermal Studies

The complexes [VO(pydx-inh)] (**1**) and [VO(pydx-nh)] (**4**) lose about 75% of their mass between 250 and 450 °C in two overlapping steps, which corresponds to the loss of the organic components minus 1.5 oxygen atoms per molecule (3 per two molecules) (calculated mass loss: 74.1%). Consequently, the remaining product is V_2O_5. The TGA profiles of the dioxovanadium(v) complexes $[K(H_2O)_3][VO_2(pydx\text{-}inh)]$ (**3**), $[K(H_2O)_3][VO_2(pydx\text{-}nh)]$ (**6**) and $[K(H_2O)_3][VO_2\text{-}(pydx\text{-}bhz)]$ (**8**) show that these complexes contain three (**3**) or two (**6** and **8**) water molecules per formula unit. The loss of this water in the temperature range 95−220 °C is indicative of coordinated water. On further increasing the temperature, the water-free species $K[VO_2(pydx\text{-}inh)]$ and $K[VO_2(pydx\text{-}nh)]$ decompose in one step between 220 and 350 °C to form KVO_3. The total loss corresponds to the loss of ligand minus 1 oxygen atom. A mass loss of 8.6%, equivalent to two water molecules (calcd. 8.93%) for **7** in the temperature range 80−135 °C, suggests that this is just water of crystallisation. Complexes **2**, **5** and the water-free form of **7** have decomposition patterns similar to those of the respective forms of **3**, **6**, and **8** after loss of water. They all yield V_2O_5 as the final product.

IR Spectroscopic Studies

The IR spectra of the ligands exhibit two bands at 3230 and 1678 [H_2pydx-inh (**I**)], 3250 and 1673 [H_2pydx-nh (**II**)] and 3210 and 1677 cm^{-1} [H_2pydx-bhz (**III**)] due to ν(NH) and ν(C=O) stretches, respectively, indicative of their ketonic nature in the solid state; cf. also Figure 1. The absence of these bands in the spectra of all complexes is consistent with enolisation and replacement of H by the metal ion. A new band appearing in the region 1220−1262 cm^{-1} is assigned to the $\nu(C-O_{enolic})$ mode. The $\nu(C=N_{azomethine})$ stretch of the free ligands appears as a weak band at 1617−1637 cm^{-1} along with the ν(C=N) stretches of the pyridine rings. A very sharp band at 1596−1608 cm^{-1} in the complexes is indicative of the coordination of the azomethine nitrogen atom. A ligand band appearing at 1017 (**I**), 1010 (**II**) and 1028 cm^{-1} (**III**) due to ν(N−N) undergoes a shift to higher wave numbers by 5−45 cm^{-1} upon complex formation. The high frequency shift of the ν(N−N)

band is expected because of diminished repulsion between the lone pairs of adjacent nitrogen atoms.[20] The ligands exhibit a medium-intensity ν(OH) band covering the region 2300−2700 cm^{-1}, which is due to intramolecular hydrogen bonds. On complexation, this band broadens and gains intensity due to the involvement of the CH_2OH group in hydrogen bonding. All of the dioxovanadium(v) complexes exhibit two or three sharp bands in the 885−950 cm^{-1} region, corresponding to the *cis*-$[VO_2]^+$ structural unit. The peroxo complexes **9** and **10** show three IR-active vibration modes associated with the peroxo moiety $[V(O_2)^{3+}]$ at 894−917, 707−717 and 553−574 cm^{-1}, which are assigned to the O−O intra-stretch (ν_1), the antisymmetric $V(O_2)$ stretch (ν_3), and the symmetric $V(O_2)$ stretch (ν_2).[21] The presence of these bands confirms the common η^2-coordination of the peroxo group.[21] In addition, both peroxo complexes exhibit an intense ν(V=O) at 946−970 cm^{-1}.

Electronic Spectra

The absorption maxima of the ligands and complexes along with their extinction coefficients are listed in Table 2. The UV spectra of H_2pydx-inh (**I**) shows three absorption bands at 216, 285.5 and 342 nm, while H_2pydx-bhz (**III**) displays four bands at 206, 296.5, 306 and 335 nm, probably belonging to the transitions φ → φ*, π → π* and *n* → π*, with the π → π* band split into two components in the case of **III**. A weak shoulder associated with the second band is traced back to association by hydrogen bonding. All of the complexes invariably showed this band, indicating the existence of hydrogen bonding in these complexes in solution as well.[22] The φ → φ* transition is only observed in the

Table 2. Electronic absorption spectra (in methanol, if not indicated otherwise)

Compound	$\lambda_{max.}$ [nm] (ε [$M^{-1}\cdot cm^{-1}$])
H_2pydx-inh (**I**)	216 (18541), 285.5 (18010), 342 (8270), 411.5 (2085)
$[VO_2$(Hpydx-inh)] (**2**) in DMF	272 (8881), 340 (7659), 421 (5769)
$[VO_2$(Hpydx-inh)] (**2**)	273 (19403), 308 (16178), 343 (16704), 416 (5073)
$[K(H_2O)_3][VO_2$(pydx-inh)] (**3**)	269.5 (18115), 337 (15146), 418 (11475)
H_2pydx-nh (**II**)	211 (23417), 307 (23898), 342 (17817)
$[VO_2$(Hpydx-nh)] (**5**)	235 (23118), 279 (16339), 328 (16322), 415 (4644)
$[K(H_2O)_2][VO_2$(pydx-nh)] (**6**)	234 (21351), 280 (16569), 326 (4384), 416 (4453)
$K[VO)(O_2)$(pydx-nh)]·H_2O (**9**)	225 (19005), 297 (15205), 308 (14622), 407 (8579)
H_2pydx-bhz (**III**)	206 (20330), 296.5 (18113), 306 (17616), 335 (11085), 406 (2106)
$[VO_2$(Hpydx-bhz)] (**4**) in DMF	270 (31939), 337 (26968), 414 (18638)
$[VO_2$(Hpydx-bhz)] (**4**)	272 (9358), 334 (5324), 407 (3164)
$[K(H_2O)_2][VO_2$(pydx-bhz)] (**8**)	237 (18304), 265 (19310), 333 (15110), 404.5 (5381)
$K[VO(O_2)$(pydx-bhz)]·H_2O (**10**)	266 (15573), 329 (11810), 424 (10282)

Table 3. ^{1}H NMR spectroscopic data

Compound[a][b]	OH (phenolic)	−CH=N−	$-CH_2-$	$-CH_3$	Aromatic H
H_2pydx-inh (**I**)	13.40 (br, 1 H)	8.15 (s,1 H)	4.76 (s, 2 H)	2.60 (s, 3 H)	9.13 (s, 1 H), 8.83 (d, 2 H), 7.99 (d, 2 H)
$[VO_2$(Hpydx-inh)] (**2**)		9.48 (s, 1 H)	4.93 (s, 2 H)	2.63 (s, 3 H)	8.90 (br, 2 H), 8.28 (s, 1 H), 8.07 (d, 2 H)
(*Δ*δ)		(1.33)			
$[K(H_2O)_3][VO_2$(pydx-inh)] (**3**)		9.10 (s, 1 H)	4.58 (s, 2 H)	2.30 (s, 3 H)	8.52 (br, 2 H), 7.91 (s, 1 H), 7.75 (d, 2 H)
(*Δ*δ)		(0.95)			
H_2pydx-nh (**II**)	13.29 (br, 1 H)	8.15 (s, 1 H)	4.76 (s, 2 H)	2.60 (s, 3 H)	9.17 (s, 1 H), 9.07 (s, 1 H), 8.81 (d, 1 H), 8.42 (d, 1 H), 7.63 (m, 1 H)
$[VO_2$(Hpydx-nh)] (**5**)		9.32 (s, 1 H)	4.83 (s, 2 H)	2.51 (s, 3 H)	8.74 (br, 1 H), 8.38 (d, 1 H), 7.89 (s, 1 H), 7.55 (m, 1 H)
(*Δ*δ)		(1.17)			
$[K(H_2O)_2][VO_2$(pydx-nh)] (**6**)		9.33 (s, 1 H)	4.89 (s, 2 H)	2.57 (s, 3 H)	9.22 (s, 1 H), 8.74 (d, 1 H), 8.40 (d, 1 H), 7.97 (s, 1 H), 7.56 (m, 1 H)
(*Δ*δ)		(1.18)			
H_2pydx-bhz (**III**)	13.14 (br, 1 H)	8.14 (s, 1 H)	4.76 (s, 2 H)	2.60 (s, 3 H)	9.09 (s, 1 H), 8.04 (d, 2 H), 7.54 (m, 3 H)
$[VO_2$(Hpydx-bhz)] (**7**)		9.28 (s, 1 H)	4.85 (s, 2 H)	2.56 (s, 3 H)	8.04 (m, 3 H), 7.49 (m, 3 H)
(*Δ*δ)	−	(1.14)			
$[K(H_2O)_2][VO_2$(pydx-bhz)] (**8**)		9.29 (s, 1 H)	4.90 (s, 2 H)	2.58 (s, 3 H)	8.10 (m, 3 H), 7.50 (m, 3 H)
(*Δ*δ)	−	(1.15)			
$K[VO(O_2)$(pydx-bhz)$H_2O]$ (**10**)		9.28 (s, 1 H)	4.89 (s, 2 H)	2.55 (s, 3 H)	8.14 (m, 3 H), 7.52 (m, 3 H)
(*Δ*δ)	−	(1.14)			

[a] Letters given in parentheses indicate the signal structure: s = singlet, d = doublet, br = broad (unresolved), m = multiplet. [b] *Δδ* = δ(complex) − δ(ligand).

oxovanadium(IV) complexes; the two other bands are significantly shifted towards lower wavelengths with respect to the uncoordinated ligands. The dioxovanadium(V) complexes are dominated by an intense band at 404.5−421 nm, which is assigned to a ligand-to-metal charge transfer (LMCT) from the phenolate oxygen atom to an empty d-orbital of the vanadium ion.

NMR Spectroscopic Studies

The coordinating modes of the ligands were confirmed by comparing ^{1}H NMR patterns of the ligands and the complexes. The relevant spectroscopic data are collected in Table 3. The broad signal appearing at δ = 13.14−13.29 ppm, due to the phenolic OH group, disappears in the spectra of the complexes. A significant downfield shift ($\Delta\delta$ = 0.84−1.33 ppm) of the signal for the azomethine (−CH=N−) proton in the complexes relative to the corresponding ligands demonstrates the coordination of the azomethine nitrogen atom. The signals due to the NH group (which is hydrogen-bonded to the alcoholic pyridoxal OH group, viz. NH···OHCH$_2$; see the structure description for **I** above) and OH protons could not be located in the δ = 0−15 ppm region in the spectra of the ligands. However, appearance of a broad signal at δ ≈ 5.8 ppm in all complexes, which we allocate to CH$_2$O*H*, suggests the breaking down of hydrogen bonding and coordination of the enolate oxygen atom of the hydrazone moiety, further supported by the absence of the NH proton signal in the complexes. The methylene and methyl protons of the pyridoxal moiety of the ligands resonate at δ = 4.76 and 2.60 ppm, and these signals appear in the complexes with slight shifts in their positions. Aromatic protons appear in the expected regions in the spectra of the ligands as well as of the complexes with minor variations in their positions. All these data are consistent with the conclusions drawn from the IR spectral studies and support the dibasic, tridentate *ONO* coordination mode.

Further characterisation of the complexes was obtained from ^{51}V NMR spectra; values of specific compounds, where solubility permitted data to be recorded, are presented in the Exp. Sect.. The resonances are somewhat broadened due to quadrupolar interaction (^{51}V: nuclear spin = 7/2, quadrupole moment = -0.05×10^{-28} m^2); the line widths at half-height are approximately 200 Hz, which is still considered comparatively narrow in ^{51}V NMR spectroscopy.[23] The dioxovanadium(V) complexes **3**, **6** and **8** show one strong resonance between δ = −532 and −534 ppm in [D$_6$]DMSO, an expected value for dioxovanadium(V) complexes having a mixed *O*/*N* donor set.[23,24] Complex **8** exhibits distinct solvent dependence. In [D$_6$]DMSO, the ^{51}V NMR signal appears at δ = −534.2 ppm, while in CH$_3$OH/CD$_3$OD it appears at δ = −546.8, possibly indicating the participation of the solvent in coordination. Similarly, the neutral dioxovanadium(V) complex **7** gives rise to a signal at δ = −535.7 ppm in [D$_6$]DMSO and at δ = −546.7 ppm in CH$_3$OH/CD$_3$OD. The peroxo complex **10** displays a ^{51}V NMR signal at δ = −586.0 ppm in [D$_6$]DMSO. This upfield shift with respect to the dioxo complexes **7** and **8** is commonly observed as an oxo group is replaced by the side-on coordinated peroxo group.[23,25]

Reaction with HCl

For the catalytic activity of vanadate-dependent haloperoxidases, the presence of a coordinated hydroxo ligand has been proposed on the basis of kinetic investigations.[6] The generation of hydroxo(oxo) species has been accomplished for [K(H$_2$O)$_2$][VO$_2$(pydx-bhz)]·H$_2$O (**8**) on reaction with HCl: Addition of HCl-saturated methanol to a methanolic solution of **8** results in a colour change from yellow to orange with gradual shift of the 404.5-nm band in the electronic absorption spectrum to 420 nm, along with a slight broadening and decrease in intensity of the absorption maximum (Figure 5). Addition of further HCl results in an increase in intensity of the 333-nm band, disappearance of the 265-nm band, and appearance of two new bands at 317 and 308 nm. In addition, a shoulder starts to appear at ca. 360 nm. The intensity and position of the 237-nm band remain constant. Corresponding results have been obtained with HClO$_4$ (dissolved in a minimum amount of methanol and added dropwise to a methanolic solution of **8**). We interpret this result in terms of the formation of an hydroxo(oxo) complex of composition [VO(OH)(H$_2$pydx-bhz)]$^{2+}$ via [VO$_2$(Hpydx-bhz)] and [VO$_2$(H$_2$pydx-bhz)]$^+$ on acidification as shown in Equation (8). The formation of the intermediate species, protonated at the pyridine nitrogen atom, viz. [VO$_2$(Hpydx-bhz)], is based on the fact that the electronic absorption spectrum of a solution of **8** obtained after addition of 4 drops of HCl nearly matches the spectrum of authentic complex **7**. The protonation of the N atom of the hydrazide moiety not involved in coordination is documented by a newly arising medium-intensity band in the IR at 3205 cm^{-1} (free Schiff base: 3210 cm^{-1}) on acidification of **8**. A comparable protonated Schiff-base complex, viz. [VO$_2$(Hsal-bhz)] (where H$_2$sal-bhz is the hydrazone derived from salicylaldehyde and benzohydrazide) has been structurally characterised.[26]

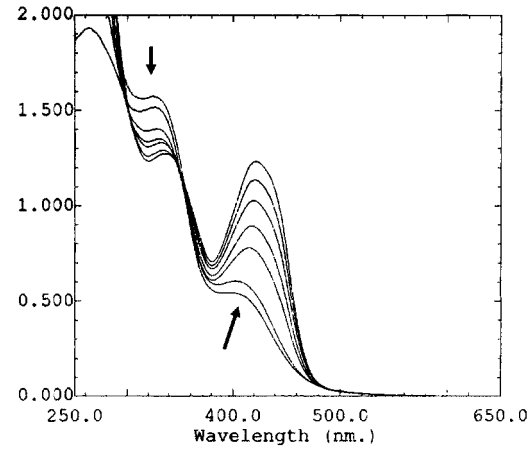

Figure 5. Titration of [K(H$_2$O)$_2$][VO$_2$(pydx-bhz)] (**8**) with a saturated solution of HCl in MeOH; the spectra were recorded after addition of 2-drops portions of MeOH/HCl to 10 mL of ca. 10^{-4} M solution of **8** in MeOH

$$\underset{\mathbf{8}}{[VO_2(pydx\text{-}bhz)]} \xrightarrow{H^+} \underset{\mathbf{7}}{[VO_2(Hpydx\text{-}bhz)]} \xrightarrow{H^+} [VO_2(H_2pydx\text{-}bhz]^+ \xrightarrow{H^+} [VO(OH)(H_2pydx\text{-}bhz)]^{2+} \quad (8)$$

Hydroxo(oxo)vanadium complexes have previously been generated on acidification of $K[VO_2(sal\text{-}inh)H_2O]$ and $[K(H_2O)_2][VO_2(Clsal\text{-}sbdt)]$ ($H_2Clsal\text{-}sbdt$ = ligand derived from salicylaldehyde and *S*-benzyldithiocarbazate).[11] An hydroxo(oxo) complex, $[VO(OH)(LH)]^+$ {where LH = *N*-(2-hydroxyethyl)-*N′*-[(*o*-hydroxyphenyl)methyl]ethylenediamine}, has been reported to form from a dinuclear dioxovanadium(v) precursor in a similar manner.[27] $[V^VO(OH)(8\text{-oxyquinolinate})_2]$[28a] and $[V^{IV}O(OH)Tp(H_2O)]$ [Tp = tris(3,5-diisopropyl-1-pyrazolyl)borate(1−)][28b] have been characterised in the solid state. On addition of a methanolic solution of KOH to $[VO(OH)(H_2pydx\text{-}bhz)]^{2+}$, the solution acquired the original spectrum of **8**; the reaction is thus reversible. This reversibility is an important observation in the context of the active-site structure and the catalytic activity of vanadate-dependent haloperoxidases, for which a hydroxo ligand at the vanadium centre has also been made plausible on the basis of X-ray diffraction data.[29]

Oxidative Bromination of Salicylaldehyde

Oxidative bromination catalysed by V_2O_5 and oxovanadium(v) complexes has been reported earlier using H_2O_2/Br^-.[30] During this process, vanadium reacts with 1 or 2 equiv. of H_2O_2, forming mono(peroxo) $[VO(O_2)^+]$ or bis(peroxo) $[VO(O_2)_2^-]$ species, which ultimately oxidise bromide, possibly by formation of a hydroperoxo intermediate. The oxidised bromine species (Br_2, Br_3^- or, most likely, HOBr) then brominates the substrate.[4,31]

We have observed that the complexes **3**, **6** and **8** satisfactorily catalyse the oxidative bromination of salicylaldehyde, using H_2O_2/KBr in the presence of $HClO_4$ in aqueous solution; cf. Equation (9). A maximum conversion of 40−46% of salicylaldehyde was found. In the case of **3** as the catalyst, GC analysis revealed the presence of three products in the ratio 8.8:86.6:4.3%, with 5-bromosalicylaldehyde being the major product. Thus, based on GC, the selectivity of the formation of 5-bromosalicylaldehyde is 86.6% with respect to salicylaldehyde conversion. On purification of the crude product by column chromatography, 5-bromosalicylaldehyde was obtained in 40% yield (related to salicylaldehyde). The average yields of pure 5-bromosalicylaldehyde for **6** and **8** as catalysts were 34.7% and 36.5%, respectively; the selectivity of formation of 5-bromosalicylaldehyde was again about 87%. In the absence of the catalyst, the reaction mixture did not produce any brominated product. Similarly, acid (here $HClO_4$) was found to be essential to carry out catalytic bromination. The complexes slowly decompose during the reaction; decomposition is slowed down, if $HClO_4$ is successively added in portions (see Exp. Sect.). Using CH_3COOH as solvent as well as the acid supplier, efficiently produced 5-bromosalicylaldehyde within 2 h of reaction time, but relatively fast decomposition of the complexes took place.

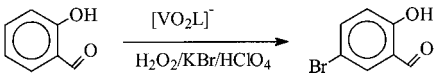

(9)

As hydroxo(oxo) species such as $[VO(OH)(H_2pydx\text{-}bhz)]^{2+}$ very likely form upon acidification of $[K(H_2O)_2][VO_2(pydx\text{-}bhz)]$ (**8**), and oxo(peroxo) species **10** are obtained upon treatment with H_2O_2 in methanol, the formation of an active oxo(peroxo) via a hydroxo(oxo) complex is likely to occur in the presence of acid as well as H_2O_2 during the catalytic reaction.[4] Activation of peroxide by coordination to vanadium may then be succeeded by formation of an intermediate hydroperoxo complex, which allows nucleophilic attack of the bromide,[21] followed by release of hypobromous acid which then brominates salicylaldehyde. A catalytic cycle is proposed in Scheme 3. It should be noted here that recent electrospray ionisation MS studies in the peroxovanadium/bromide system indicated the formation of a hypobromite species, $[VO(OH)(H_2O)_3OBr]^+$, the stability of which is supported by ab initio calculations.[32]

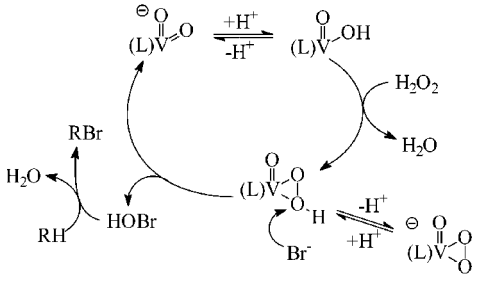

Scheme 3

Conclusion

Pentacoordinated neutral and cationic dioxovanadium complexes containing a ligand system providing a dianionic *ONO* donor set and thus modelling the active site of vanadate-dependent haloperoxidases have been synthesised and characterised. The cationic complexes of the general composition $[K(H_2O)_n][VO_2(ONO)]$ can be converted in situ on acidification to hydroxo(oxo) complexes $[VO(OH)(H_2ONO)]^{2+}$ and to the peroxo complexes $K[VO(O_2)(ONO)]$, and thus to species assumed to be intermediates in the bromoperoxidase activity of the enzymes. The complexes are in fact active in bromination of salicylaldehyde in the presence of H_2O_2, Br^- and acid, and hence may also be considered *functional* models. The *ONO* ligands employed are hydrazones containing pyridoxal (vitamin B_6) and nicotinohydrazides as components, and thus biogenic molecular moieties.

The complex $[K(H_2O)_3][VO_2(pydx\text{-}inh)]$ (where pydx-inh is the doubly deprotonated condensation product from

pyridoxal and isonicotinohydrazide), which has been structurally characterised, contains the ligand in the enolate form (the free ligand constitutes the ketonic form). The seven-coordinate potassium ion links to three different $[VO_2(pydx\text{-}inh)]^-$ anions and thus generates, together with hydrogen bonds, a complex supramolecular, three-dimensional network.

Experimental Section

Materials and Instrumentation: V_2O_5, NH_4VO_3, isonicotinohydrazide, benzoyl chloride, hydrazine hydrate (Loba Chemie, India), pyridoxal hydrochloride (Fluka Chemie, GmbH, Switzerland), acetylacetone (Hacac) (Aldrich, U.S.A.), and 30% aqueous H_2O_2 (Qualigens, India) were used as obtained. Other chemicals and solvents were of analytical reagent grade. Benzohyrazide was prepared by the reaction of a twofold excess of hydrazine hydrate with ethyl benzoate, which in turn was obtained by refluxing benzoyl chloride in an excess of absolute ethanol. $[VO(acac)_2]$ was prepared according to the method reported in the literature.[33] The microanalytical section of the Central Drug Research Institute, Lucknow, India, performed elemental analyses of the ligands and complexes. IR spectra were recorded as KBr pellets with a Perkin−Elmer model 1600 FT-IR spectrometer. Electronic absorption spectra were measured in methanol or DMF with a UV-1601 PC UV/Vis spectrophotometer. ^{1}H NMR spectra were obtained with a Bruker 200, and ^{51}V NMR spectra with a Bruker Avance 400 MHz spectrometer at 94.73 MHz with the common parameter settings. NMR spectra were usually recorded in $[D_6]$DMSO, and $\delta(^{51}V)$ values are quoted relative to $VOCl_3$ as external standard. Selected ^{51}V NMR spectroscopic results have also been obtained in CD_3OD. Thermogravimetric analyses of the complexes were carried out under oxygen using a TG Stanton Redcroft STA 780 instrument. Magnetic susceptibility measurements of oxovanadium(IV) complexes were carried out at room temperature by the Scientific Instrumentation Centre of the Indian Institute of Technology in Roorkee. EPR spectra were recorded with a Bruker ESP 300E spectrometer between 9.42 and 9.47 GHz, and EPR parameters were adjusted by simulation with the Bruker program system SimFonia. All reaction products obtained from the catalytically conducted reactions were identified by recording their m.p., ^{1}H NMR and IR spectra after purification and separation by column chromatography on silica gel using CH_2Cl_2 as an eluant. The product mixture obtained before purification was additionally analysed with a Shimadzu 14B gas chromatograph, fitted with an SE-52 packed column, coupled with an FID detector, and the identity of the products confirmed by checking against the GC-MS reference system Shimadzu QP-5000. Crystal structure data were collected with a Bruker SMART Apex CCD diffractometer, using graphite-monochromated Mo-K_α radiation (λ = 0.71073 Å) at 153(2) K. In the case of ligand **I**, all hydrogen atoms (except H3A) were placed into calculated positions and included in the last cycles of refinement. H3A of ligand **I** and all H atoms of complex **3** were found. The program systems SHELXS 86 and SHELXL 93 were used throughout. Crystal data and details of the data collection and refinement are collated in Table 4. CCDC-233587 (**I**) and −233586 (**3**) contain the supplementary crystallographic data of this paper. These data can be obtained free of charge at www.ccdc.cam.ac.uk/conts/retrieving/

Table 4. Crystal and refinement data for complex **3** and ligand **I**

	3	**I**
Empirical formula	$C_{14}H_{10}KN_4O_8V$	$C_{14}H_{15}N_4O_3$
Formula mass [g·mol^{-1}]	452.30	287.30
Crystal system	triclinic	monoclinic
Space group	*Pi*	*P*21/*n*
Unit cell dimensions:		
a [Å]	7.3320(4)	8.0828(5)
b [Å]	10.9605(6)	12.9614(9)
c [Å]	12.6229(7)	12.9926(8)
α [°]	64.7210(10)	90
β [°]	81.113(2)	90.5000(10)
γ [°]	89.366(2)	90
V [Å^3]	904.54(9)	1361.11(15)
Z	2	3
Calculated density [g·cm^{-3}]	1.661	1.397
Absorption coefficient [mm^{-1}]	0.830	0.102
F(000)	456	600
Crystal size [mm]	0.80 × 0.22 × 0.12	0.43 × 0.29 × 0.19
θ range for data collection [°]	2.06 to 32.56	2.22 to 28.00
Index ranges	$-10 \le h \le 10$	$-10 \le h \le 10$
	$-16 \le k \le 16$	$-16 \le k \le 17$
	$-19 \le l \le 19$	$-17 \le l \le 16$
Reflections collected	24828	16031
Independent reflections	6380 [*R*(int) = 0.0435]	3182 [*R*(int) = 0.0409]
Completeness to θ [°]	97.0%	96.6%
Data/restraints/parameters	6380/0/293	3182/0/192
Goodness-of-fit on F^2	1.052	1.111
Final *R* indices [$I > 2\sigma(I_0)$]	*R*1 = 0.0400, *wR*2 = 0.1178	*R*1 = 0.0608, *wR*2 = 0.1330
R indices (all data)	*R*1 = 0.0453, *wR*2 = 0.1206	*R*1 = 0.0818, *wR*2 = 0.1523
Largest difference peak/hole [e Å^{-3}]	0.936/−0.439	0.631/−0.623

html or from the Cambridge Crystallographic Data Centre, 12 Union Road, Cambridge CB2 1EZ, UK [Fax: (internat.) + 44-1223-336-033; E-mail: deposit@ccdc.cam.ac.uk].

Preparation of Ligands

H_2pydx-inh (I): A mixture of pyridoxal hydrochloride (1.02 g, 5 mmol) and isonicotinohydrazide (0.685 g, 5 mmol) in 50 mL of methanol was refluxed using a water bath for 4 h. After reducing the solvent volume to ca. 15 mL, the mixture was cooled to room temperature within 3 h. During this time, a light orange solid of **I** precipitated, which was filtered off, washed with methanol and dried. **I** was recrystallised from methanol to give a crystalline solid. Yield 1.15 g (81%). $C_{14}H_{14}N_4O_3$ (286.3): calcd. C 58.74, H 4.90, N 19.58; found C 58.69, H. 4.82, N 19.41. IR (KBr): $\tilde{\nu}_{max.}$ = 3230 (NH), 1678 (C=O), 1620, 1600 (ring C=N and C=N), 1017 (N−N) cm^{-1}.

H_2pydx-nh (II) and H_2pydx-bhz (III): These ligands were prepared according to the procedure outlined for **I**.

II: Yield 1.12 g (78%). $C_{14}H_{14}N_4O_3$ (286.3): calcd. C 58.74, H 4.90, N 19.58; found C 58.82, H 4.85, N 19.48. IR (KBr): $\tilde{\nu}_{max.}$ = 3250 (NH), 1673 (C=O), 1617 (ring C=N, C=N), 1025 (N−N) cm^{-1}.

III: Yield 1.07 g (75%). $C_{15}H_{15}N_3O_3$ (285.3): calcd. C 63.18, H 5.26, N 14.74; found C 63.00, H, 5.34, N 14.68. IR (KBr): $\tilde{\nu}_{max.}$ = 3210 (NH), 1677 (C=O), 1637, 1624 (ring C=N, C=N), 1045 (N−N) cm^{-1}.

Preparation of Complexes

[VO(pydx-inh)] (1) and [VO_2(Hpydx-inh)] (2): A stirred solution of H_2pydx-inh (0.570 g, 0.002 mol) in dry methanol (20 mL) was treated with [VO(acac)$_2$] (0.530 g, 0.002 mol), dissolved in dry methanol (10 mL), and the resulting reaction mixture was refluxed using a water bath for 5 h. After cooling to room temperature, a brown precipitate of **1** was filtered off, washed with methanol and dried. Compound **1** was suspended in methanol (50 mL), and air was slowly passed through the suspension at ca. 40 °C for ca. 24 h with occasional shaking. During this period of time, the brown suspension slowly disappeared and crystalline orange-red solid **2** separated. This was filtered off, washed with methanol and dried in vacuo. For the direct preparation of **2**, it is not necessary to isolate **1**.

Data for 1: Yield 0.35 g (50%). $C_{14}H_{12}N_4O_4V$ (351.2): calcd. C 47.86, H 3.42, N 15.95; found C 47.43, H 3.61, N 15.86. IR (KBr): $\tilde{\nu}_{max.}$ = 1601 (C=N), 1262 (C−O, enolate), 1060 (N−N), 888 (V=O) cm^{-1}. EPR (DMSO, 98 K): g_{xy} = 1.984, g_z = 1.949; A_{xy} = 55.1, A_z = 159.7 × 10^{-4} cm^{-1}.

Data for 2: Yield 0.48 g (65%) based on [VO(acac)$_2$]. $C_{14}H_{13}N_4O_5V$ (368.2): calcd. C 45.65, H 3.53, N 15.22; found C 45.39, H 3.72, N 15.44. IR (KBr): $\tilde{\nu}_{max.}$ = 1599 (C=N), 1257 (C-O, enolate), 1055 (N−N), 956, 908 (sym. and antisym. VO_2^+) cm^{-1}.

[$K(H_2O)_3$][VO_2(pydx-inh)] (3): Vanadium(v) oxide (0.91 g, 0.005 mol) was suspended in aqueous KOH (0.30 g, 0.005 mol in 10 mL H_2O) and stirred with occasional heating at 50 °C for 2 h. The potassium vanadate solution thus generated was filtered. A filtered solution of H_2pydx-inh (1.42 g, 0.005 mol), dissolved in 20 mL of aqueous KOH (0.56 g, 0.010 mol), was added with stirring, and the pH of the reaction mixture was cautiously adjusted to 7.5 with 4 M HCl. After 2 h of stirring, the precipitated yellow solid was filtered off, washed with water followed by acetone, and dried. On crystallisation from ca. 50 mL of methanol, **2** precipitated as an orange-red solid, which was filtered off and dried in vacuo over silica gel. For the data of **2**, see above. After reducing the volume of the filtrate to ca. 15 mL and keeping it at ca. 10 °C, yellow crystalline **3** slowly precipitated within 2 d. This was filtered off, washed with cold methanol and dried. Yield 1.58 g (68%). $C_{14}H_{18}KN_4O_8V$ (460.4): calcd. C 36.52, H 3.91, N 12.17; found C 36.33, H 3.85, N 12.26. IR (KBr): $\tilde{\nu}_{max.}$ = 1596 (C=N), 1257 (C−O, enolate), 1055 (N−N), 955, 909 (sym. and antisym. VO_2^+) cm^{-1}. ^{51}V NMR ([D_6]DMSO): δ = −532.0 ppm.

[VO(pydx-nh)] (4) and [VO_2(Hpydx-nh)] (5): Complex **4** was prepared analogously to **1**, replacing H_2pydx-inh for H_2pydx-nh. Air was slowly passed through the methanolic suspension (50 mL) of **4** at ca. 40 °C for ca. 24 h with occasional shaking. After cooling to ca. 10 °C for 2 d, yellow crystalline **5** slowly preciptated, which was filtered, washed with methanol and dried in vacuo.

Data for 4: Yield 0.61 g (86.8%). $C_{14}H_{12}N_4O_4V$ (351.2): calcd. C 47.86, H 3.42, N 15.95; found C 47.94, H 3.31, N 15.98. IR (KBr): $\tilde{\nu}_{max.}$ = 1608 (C=N), 1248 (C−O, enolate), 1050 (N−N), 888 (V=O) cm^{-1}. EPR (DMSO, 98 K): g_{xy} = 1.984, g_z = 1.942; A_{xy} = 56.7, A_z = 161.2 × 10^{-4} cm^{-1}.

Data for 5: Yield 0.40 g (54%) based on VO(acac)$_2$. $C_{14}H_{13}N_4O_5V$ (368.2): calcd. C 45.65, H 3.53, N 15.22; found C 45.83, H 3.36, N 15.17. IR (KBr): $\tilde{\nu}_{max.}$ = 1597 (C=N), 1234(C−O, enolate), 1064 (N−N), 961, 942, 884 (sym. and antisym. VO_2^+) cm^{-1}.

[$K(H_2O)_2$][VO_2(pydx-nh)] (6): This complex was prepared from KVO_3 and H_2pydx-nh by the method outlined for **3**. The crude mass obtained on crystallisation from methanol gave a 1.45 g (66%) yield of **6**. $C_{14}H_{16}KN_4O_7V$ (417.3): calcd. C 38.01, H 3.65, N 12.67; found C 38.20, H 3.74, N 12.56. IR (KBr): $\tilde{\nu}_{max.}$ = 1606 (C=N), 1258 (C−O, enolate), 1042 (N−N), 940, 923 (sym. and antisym. VO_2^+) cm^{-1}. ^{51}V NMR ([D_6]DMSO): δ = −532.0 ppm.

[VO_2(Hpydx-bhz)]·2H_2O (7): A stirred solution of H_2pydx-bhz (0.570 g, 2 mmol) in methanol (20 mL) was treated with [VO(acac)$_2$] (0.530 g, 2 mmol), and the reaction mixture was refluxed using a water bath for 5 h to give a brown solution. After cooling to ambient temperature, a current of air was passed through this solution for ca. 20 h; during this procedure, yellow complex **7** slowly precipitated. This was filtered off, washed with methanol and dried in vacuo. Yield 0.68 g (84%) based on [VO(acac)$_2$]. $C_{15}H_{18}N_3O_7V$ (403.3): calcd. C 44.66, H 4.47, N 10.42; found C 44.75, H 4.36, N 10.28. IR (KBr): $\tilde{\nu}_{max.}$ = 1599 (C=N), 1220 (C−O, enolate), 1063 (N−N), 940, 918, 888 (sym. and antisym. VO_2^+) cm^{-1}. ^{51}V NMR: δ: −535.7 ppm ([D_6]DMSO); −546.4 ppm (MeOH/CD_3OD).

[$K(H_2O)_2$][VO_2(pydx-bhz)] (8): Complex **8** was prepared from KVO_3 (generated in solution from V_2O_5 and KOH) according to the procedure outlined for **3**. Recrystallisation from methanol gave **8** in pure form as a yellow crystalline material. Yield 1.48 g (66%). $C_{15}H_{17}KN_3O_7V$ (441.4): 40.82, C 3.88, N 9.52; found C 40.73, H 3.97, N 9.41. IR (KBr): $\tilde{\nu}_{max.}$ = 1597 (C=N), 1222 (C−O, enolate), 1063 (N−N), 938, 915, 888 (sym. and antisym. VO_2^+) cm^{-1}. ^{51}V NMR: δ = −534.2 ppm ([D_6]DMSO); −546.9 ppm (MeOH/CD_3OD).

K[$VO(O_2)$(pydx-nh)]·H_2O (9): Complex **6** (900 mg, 2 mmol), dissolved in 20 mL of MeOH, was treated with 30% aqueous H_2O_2 (3 mL, 26.5 mmol) while stirring the reaction mixture at 10 °C, which caused darkening of the solution. After 2 h of stirring, the volume was reduced to ca. 10 mL and the solution was kept at 10 °C overnight. Yellow crystals precipitated, which were filtered off and dried in vacuo. Yield 0.30 g (34%). $C_{14}H_{14}KN_4O_7V$ (440.33): calcd. C 38.19, H 3.20, N 12.72; found C 38.0, H 3.33, N 12.61. IR (KBr): $\tilde{\nu}_{max.}$ = 1603 (C=N), 1250 (C−O, enolate), 1043 (N−N),

946 (V=O), 894 (O−O), 707 [$V(O_2)$ antisym.], 574 [$V(O_2)$ sym.] cm^{-1}.

K[$VO(O_2)$(pydx-bhz)]·H_2O (10). Method 1: A 30% aqueous solution of H_2O_2 (2 mL, 17.6 mmol) was added to an aqueous solution of KVO_3 (2 mmol), prepared as outlined above. The potassium salt of H_2pydx-bhz was prepared separately by treating **III** (0.570 g, 2 mmol) with KOH (0.168 g, 3 mmol) in water (10 mL) followed by filtration. This solution was added dropwise to the above solution with constant stirring. After 2 h of stirring, the orange solid that had precipitated was filtered, washed with water and dried. The crude mass was recrystallised from methanol. Yield 0.14 g (16%). **Method 2:** This method parallels the one adopted for **9**, using **8** and H_2O_2. Yield 0.48 g (22%). $C_{15}H_{15}KN_3O_7V$ (439.3): calcd. 41.01, H 3.44, N 9.56; found C 40.87, H 3.41, N 9.45. IR (KBr): $\tilde{\nu}_{max.}$ = 1596 (C=N), 1246 (C−O, enolate), 1033 (N−N), 970 (V=O), 917 (O−O), 717 [$V(O)_2$ antisym.], 553 [$V(O)_2$ sym.] cm^{-1}. ^{51}V NMR ([D_6]DMSO): $\delta = -536.0$ ppm.

Reactions of 9 and 10 with PPh_3: PPh_3 (0.39 g, 1.5 mmol) was added to complex **9** or **10** (1 mmol), dissolved in dry methanol (20 mL), and the reaction mixture heated under reflux for 8 h. After reduction of the volume to ca. 10 mL, the solution was kept at 10 °C to yield a yellow precipitate. This was filtered, washed with methanol and dried in vacuo. Yield ca. 50%. The analytical and spectroscopic data of the complexes thus obtained match well with those of **6** and **8**, respectively. The formation of $OPPh_3$ was documented by ^{31}P NMR spectroscopy.

Catalytic Oxidative Bromination of Salicylaldehyde: In a typical reaction, salicylaldehyde (0.244 g, 2 mmol) was added to an aqueous solution of KBr (0.5 g, 4 mmol, in 4 mL H_2O), followed by addition of aqueous 30% H_2O_2 (1.93 g, 15 mmol). This mixture was treated whilst stirring with the catalyst (0.02 g) and 70% $HClO_4$ (1 mmol). Addiditional 1-mmol portions of $HClO_4$ were added during the course of the reaction every hour. After 4 h of reaction time, the white precipitate that had formed was filtered off, washed with water followed by diethyl ether, and dried. The crude mass was dissolved in CH_2Cl_2, and insoluble material, if any, was removed by filtration. The filtrate was concentrated to ca. 5 mL and chromatographed on silica gel (column dimensions 30 × 2.5 cm) with CH_2Cl_2 as eluant. The first fraction was collected and the solvents were evaporated to dryness to give 5-bromosalicylaldehyde. Alternatively, the filtered dichloromethane solution of the crude material was analysed by GC-MS.

Acknowledgments

We acknowledge the performance of the microanalyses by the Regional Sophisticated Instrumental Centre, CDRI, Lucknow, and financial assistance from the Department of Science and Technology, Government of India (Grant No. SP/S1/F-07/2001), New Delhi, and the Deutsche Forschungsgemeinschaft (grant RE 431/13-4).

[1] M. R. Maurya, *Coord. Chem. Rev.* **2003**, *237*, 163−181.
[2] D. Rehder, *Inorg. Chem. Commun.* **2003**, *6*, 604−617.
[3] [3a] K. H. Thompson, J. H. McNeill, C. Orvig, *Chem. Rev.* **1999**, *99*, 2561−2571. [3b] H. Sakurai, Y. Kojima, Y. Yoshikawa, K. Kawabe, H. Yasui, *Coord. Chem. Rev.* **2002**, *226*, 187−198. [3c] D. Rehder, J. Costa Pessoa, C. F. G. C. Geraldes, M. M. C. A. Castro, T. Kabanos, T. Kiss, B. Meier, G. Micera, L. Pettersson, M. Rangel, A. Salifoglou, I. Turel, D. Wang, *J. Biol. Inorg. Chem.* **2002**, *7*, 384−396.
[4] A. Butler, *Coord. Chem. Rev.* **1999**, *187*, 17−25.
[5] [5a] M. Weyand, H.-J. Hecht, M. Kieß, M.-F. Liaud, H. Vilter, D. Schomburg, *J. Mol. Biol.* **1999**, *293*, 595−611. [5b] M. I. Isupov, A. R. Dalby, A. A. Brindley, Y. Izumi, T. Tanabe, G. N. Murshudov, J. A. Littlechild, *J. Mol. Biol.* **2000**, *299*, 1035−1049. [5c] A. Messerschmidt, R. Wever, *Proc. Natl. Acad. Sci. U. S. A.* **1996**, *93*, 392−396.
[6] [6a] G. J. Colpas, B. J. Hamstra, J. W. Kampf, V. L. Pecoraro, *J. Am. Chem. Soc.* **1996**, *118*, 3469−3478. [6b] B. J. Hamstra, G. J. Colpas, V. L. Pecoraro, *Inorg. Chem.* **1998**, *37*, 949−955.
[7] H. B. ten Brink, H. E. Schoemaker, R. Wever, *Eur. J. Biochem.* **2001**, *268*, 132−138.
[8] [8a] C. Bolm, F. Bienewald, *Angew. Chem. Int. Ed. Engl.* **1996**, *34*, 2640−2642. [8b] G. Santoni, G. M. Licini, D. Rehder, *Chem. Eur. J.* **2003**, *9*, 4700−4708. [8c] T. S. Smith II, V. L. Pecoraro, *Inorg. Chem.* **2002**, *41*, 6750−6760.
[9] [9a] K. Kimplin, X. Bu, A. Butler, *Inorg. Chem.* **2002**, *41*, 161−163. [9b] M. Časný, D. Rehder, *Chem. Commun.* **2001**, 921−922.
[10] A. Messerschmidt, L. Prade, R. Wever, *Biol. Chem.* **1997**, *378*, 309−315.
[11] [11a] M. R. Maurya, S. Khurana, C. Schulzke, D. Rehder, *Eur. J. Inorg. Chem.* **2001**, 779−787. [11b] M. R. Maurya, S. Khurana, W. Zhang, D. Rehder, *J. Chem. Soc., Dalton Trans.* **2002**, 3015−3023. [11c] M. R. Maurya, S. Khurana, W. Zhang, D. Rehder, *Eur. J. Inorg. Chem.* **2002**, 1749−1760.
[12] M. R. Maurya, S. Khurana, D. Rehder, *Trans. Met. Chem.* **2003**, *28*, 511−517.
[13] W. Plass, *Coord. Chem. Rev.* **2003**, *237*, 205−212.
[14] C. C. Lee, A. Syamal, L. J. Theriot, *Inorg. Chem.* **1971**, *10*, 1669−1672.
[15] [15a] C. J. Carrano, C. M. Nun, R. Quan, J. A. Bonadies, V. L. Pecoraro, *Inorg. Chem.* **1990**, *29*, 944−951. [15b] D. Schulz, T. Weyhermüller, K. Wieghardt, B. Nuber, *Inorg. Chim. Acta* **1995**, *240*, 217−229. [15c] J. Costa Pessoa, J. A. L. Silva, A. L. Vieira, L. Vilas-Boas, P. O'Brien, P. Thornton, *J. Chem. Soc., Dalton Trans.* **1992**, 1745−1749. [15d] S. Mondal, P. Ghosh, A. Chakravorty, *Inorg. Chem.* **1997**, *36*, 59−63. [15e] C. Grüning, H. Schmidt, D. Rehder, *Inorg. Chem. Commun.* **1999**, *2*, 57−59.
[16] N. Julien-Cailhol, E. Rose, J. Vaisserman, D. Rehder, *J. Chem. Soc., Dalton Trans.* **1996**, 2111−2121.
[17] [17a] A. J. Tasiopoulos, A. N. Troganis, A. Evangelou, C. P. Raptopoulos, A. Terzis, Y. Deligiannakis, T. A. Kabanos, *Chem. Eur. J.* **1999**, 910−921. [17b] T. S. Smith II, R. LoBrutto, V. L. Pecoraro, *Coord. Chem. Rev.* **2002**, *228*, 1−18.
[18] K. Elvingson, A. Gonzáles-Baró, L. Pettersson, *Inorg. Chem.* **1996**, *35*, 3388−3393.
[19] [19a] C. R. Cornman, K. M. Geiser-Bush, S. P. Rowley, P. D. Boyle, *Inorg. Chem.* **1997**, *36*, 6401−6408. [19b] G. Santoni, G. Licini, D. Rehder, *Chem. Eur. J.* **2003**, *9*, 4700−4708.
[20] S. P. Perlepes, D. Nicholls, M. R. Harison, *Inorg. Chim. Acta* **1985**, *102*, 137−143.
[21] [21a] A. D. Westland, F. Haque, J.-M. Bouchard, *Inorg. Chem.* **1980**, *19*, 2255−2259. [21b] M. Časný, D. Rehder, *Dalton Trans.* **2004**, 839−846. [21c] M. Sivák, M. Mad'orová, J. Taatiersky, J. Marek, *Eur. J. Inorg. Chem.* **2003**, 2075−2081.
[22] A. T. T. Hsieh, R. M. Sheahan, B. O. West, *Aust. J. Chem.* **1975**, *28*, 885−891.
[23] [23a] D. Rehder, C. Weidemann, A. Duch, W. Priebsch, *Inorg. Chem.* **1988**, *27*, 584−587. [23b] D. Rehder, *Transition Metal Nuclear Magnetic Resonance* (Ed.: P. S. Pregosin), Elsevier, New York **1991**, pp. 1−58.
[24] O. W. Howarth, *Progr. Magn. Reson. Spetrosc.* **1990**, *22*, 453−485.
[25] I. Andersson, S. Angus-Dunne, O. Howarth, L. Pettersson, *J. Inorg. Biochem.* **2000**, *80*, 51−58.
[26] W. Plass, A. Pohlmann, H.-K. Yozgatli, *J. Inorg. Biochem.* **2000**, *80*, 181−183.
[27] G. J. Colpas, B. J. Hamstra, J. W. Kampf, V. L. Pecoraro, *Inorg.*

Chem. **1994**, *33*, 4669−4675.
[28] [28a] A. Giacomelli, C. Floriani, A. O. De Souza Duarte, A. Chiesi-Villa, C. Guastino, *Inorg. Chem.* **1982**, *21*, 3310−3316. [28b] M. Kosugi, S. Hikichi, M. Akita, Y. Moro-oka, *Inorg. Chem.* **1999**, *38*, 2567−2578.
[29] [29a] A. Messerschmidt, L. Prade, R. Wever, *Biol. Chem.* **1997**, *378*, 309−315. [29b] S. Macedo-Ribeiro, W. Hemrika, R. Renirie, R. Wever, A. Messerschmidt, *J. Biol. Inorg. Chem.* **1999**, *4*, 209−219.
[30] A. G. J. Ligtenbarg, R. Hage, B. L. Feringa, *Coord. Chem. Rev.* **2003**, *237*, 89−101.
[31] [31a] A. Butler, in *Bioinorganic Catalysis* (Eds.: J. Reedijk, E. Bouwman), 2nd ed., Marcel Dekker, New York **1999**, chapter 5. [31b] V. L. Pecoraro, C. Slebodnick, B. Hamstra, in *Vanadium Compounds: Chemistry, Biochemistry and Therapeutic Applications* (Eds.: D. C. Crans, A. S. Tracy), ACS Symposium Series, American Chemical Society, Washington, **1998**, chapter 12.
[32] O. Bortolini, M. Carrano, V. Conte, S. Moro, *Eur. J. Inorg. Chem.* **2003**, 42−46.
[33] R. A. Row, M. M. Jones, *Inorg. Synth.* **1957**, *5*, 113−116.

Received March 15, 2004
Early View Article
Published Online November 4, 2004

